DOE-ET-53088-249 IFSR#249

WAKELESS TRIPLE SOLITON ACCELERATOR

*K. Mima,** *T. Ohsuga,** *H. Takabe,** *K. Nishihara**,
T. Tajima, *E. Zaidman*, and *W. Horton*
Institute for Fusion Studies
The University of Texas at Austin
Austin, Texas 78712-1060

* Inst. of Laser Eng., Osaka University, Osaka 565 Japan

September 1986

Wakeless Triple Soliton Accelerator

K. Mima, T. Ohsuga, H. Takabe, and *K. Nishihara*

Institute of Laser Engineering

Osaka University

Suita, Osaka 565 Japan

and

T. Tajima, E. Zaidman and *W. Horton*

Institute for Fusion Studies and Department of Physics

The University of Texas at Austin

Austin, Texas 78712-1081

Abstract

We introduce and analyze the concept of a wakeless triple soliton accelerator in a plasma fiber. Under appropriate conditions the triple soliton with two electromagnetic and one electrostatic waves in the beat-wave resonance propagates with velocity c leaving no plasma wake behind, while the phase velocity of the electrostatic wave is made also c in the fiber.

The pump power depletion in the ultra-high energy accelerator is a severe problem. Its severity may be appreciated by considering the desired luminosity $\mathcal{L}$. Since the relevant cross-section σ decreases inversely proportional to the square of the center-of-mass energy $E_{\rm cm}$, the luminosity $\mathcal{L}$ has to increase as $\mathcal{L} \propto E_{cm}^2$, (e.g., $\mathcal{L} = 10^{34} cm^{-2}\,\mathrm{sec}^{-1}$ at 10TeV e^+e^-)[1], in order to keep the number of relevant events constant in a given time, and thus the necessary power supplied to an accelerator $P \propto E_{cm}^2$. In the beat-wave accelerator,[2] however, the pump depletion problem is uniquely important and possibly quite damaging. This is because the accelerating electrostatic beat wave propagates with group velocity close to zero, i.e., $3(v_e/c)v_e$ with v_e being the electron thermal velocity, while the laser beams propagate approximately with the speed of light c. Thus the laser beams that enter the fresh plasma expend their energy in creating the plasma wave that is left out in the laboratory (plasma rest frame) behind the pump beams. Thus the beat wave accelerator would suffer greatly from this heavy pump depletion in addition to the already severe pump power requirement.

In this Letter we introduce the idea of wakeless triple soliton acceleration in order to overcome this difficulty, and analyze this idea for its plausibility as an accelerator concept. The essence of our idea is to use the self-induced transparency due to the plasma nonlinearity and deliberately shaped optical beams, to drive a triple soliton accelerating structure without a wake. A phenomenon similar to this was discovered in nonlinear crystals.[3] A triple soliton is a "vector soliton" composed of two transverse electromagnetic potentials and one electrostatic potential, while the conventional plasma soliton is a "scalar soliton" composed of one electrostatic potential.[4]

The coupled three-wave equations for the beat wave excitation are given by

$$\left(\frac{\partial}{\partial t} + v_{g_0}\frac{\partial}{\partial x}\right)\phi_0 = \beta_0\phi_1\phi_p^*, \tag{1}$$

$$\left(\frac{\partial}{\partial t} + v_{g_1}\frac{\partial}{\partial x}\right)\phi_1 = -\beta_1\phi_0\phi_p^*, \tag{2}$$

$$\left[\frac{\partial}{\partial t} + v_{gp}\frac{\partial}{\partial x} - i\Delta\omega - \frac{3i}{16}\omega_p|\phi_p|^2\right]\phi_p = -\beta_p\phi_0\phi_1^*, \tag{3}$$

where $\beta_0 = \omega_p^2/2\omega_0$, $\beta_1 = \omega_p^2/2\omega_1$, $\beta_p = \omega_p/2$, and v_{gj} is the group velocities of electromagnetic and electrostatic waves. The frequency mismatch is $\Delta\omega = \omega_0 - \omega_1 - \omega_p$. Note that the fourth term on the left-hand side of Eq. (3) is the nonlinear frequency shift associated with the electron relativistic-mass correction[5] which limits the amplitude of the ideal plasma wave growth to $eE_p/m\omega_p = (16/3)^{1/3}(\phi_0\phi_1)^{1/3}$. The mode coupling equations (1)-(3) conserve two action integrals and the interaction Hamiltonian.[6] This integrable system contains soliton solutions.[7]

In Eqs. (1)-(3) the complex amplitudes $\phi_j(x,t)$'s are slowly varying functions of x and t such that $eE_j/mc\omega_j = v_j/c = \frac{1}{2}\phi_j(x,t)\exp[i(k_jx - \omega_jt)] + \text{c.c.}$ ($j = 0, 1,$ or p). Looking for a stationary structure $\phi_j(\xi = x - \lambda t)$ traveling with speed λ, we have

$$\frac{d}{d\xi}\phi_0 = -\tilde{\beta}_0\phi_1\phi_p, \tag{4}$$

$$\frac{d}{d\xi}\phi_1 = \tilde{\beta}_1\phi_0\phi_p^*, \tag{5}$$

$$\left(\frac{d}{d\xi} + i\Delta\tilde{\omega} + i\tilde{\Lambda}\right)\phi_p = \tilde{\beta}_p\phi_0\phi_1^*, \tag{6}$$

where $\tilde{\Lambda} = (3\omega_p/16)|\phi_p|^2/(\lambda - v_{gp})$, $\tilde{\beta}_j = \beta_j/(\lambda - v_{gj})$ ($j = 0, 1$ or p) and $\Delta\tilde{\omega} = \Delta\omega/(\lambda - v_{gp})$.

When the relativistic nonlinear frequency shift $\tilde{\Lambda}$ is neglected and $\Delta\tilde{\omega} = 0$, the exact solutions to Eqs. (4)-(6) are $\phi_0^2 = a^2 sn^2\left[-\sqrt{\tilde{\beta}\tilde{\beta}_p}\xi, a/b\right]$, $\phi_1^2 = b^2 - \phi_0^2$ and $\phi_p^2 = \left(\tilde{\beta}_p/\tilde{\beta}\right)a^2\left[1 - \phi_0^2/a^2\right]$. Here, we approximated $\tilde{\beta}_0 = \tilde{\beta}_1 = \tilde{\beta}$ and $v_{g0} = v_{g1} = v_g$ for $\omega_0 \gg \omega_p$. When a=b, we have the triple soliton solution,

$$\phi_0 = -a\tanh\ q(x - \lambda t) \tag{7}$$

$$\phi_1 = a\ \text{sech}\ q(x - \lambda t) \tag{8}$$

$$\phi_p = a_p\ \text{sech}\ q(x - \lambda t) \tag{9}$$

where $q = \sqrt{\tilde{\beta}\tilde{\beta}_p}a$ and

$$\lambda = \left(v_g - v_{gp}\beta a_p^2/\beta_p a^2\right) \Big/ \left[1 - \left(\beta a_p^2/\beta_p a^2\right)\right]. \tag{10}$$

Note that the electromagnetic and electrostatic envelopes have the same characteristic wavenumber q and the phase velocity λ, hence the name of the triple soliton. The speed λ of the triple soliton is a function of a and β, which can be tuned to be the speed of light when $\frac{a_p}{a} = \frac{1}{\sqrt{2}}\left(\frac{\omega_p}{\omega_0}\right)^{1/2}$. Physically, the three envelopes phase lock such that phase $(\phi_0\phi_1^*) = 0$ in $x > \lambda t$ (the pulse front) and the amplitude of the higher frequency pulse decreases in time as the lower side-bands ϕ_1 and ϕ_p are excited through (5) and (6). Around the pulse center ($x \simeq \lambda t$) the phase of the pump wave ϕ_0 jumps by π and thus the inverse decay process begins. Namely, ϕ_0 increases and the energy in ϕ_p is restored back to ϕ_0 as shown in Fig. 1(a).

Generalizations of the trisoliton solutions (7)-(10) are possible. First, we find that $\phi_p(x,t) \to 0$ for $|x| \to \infty$ i.e., no wake is created, if $\int_{-\infty}^{\infty} \phi_0(\xi)\phi_1^*(\xi)d\xi$ vanishes. When there is a substantial relativistic detuning, this effect may be compensated for by a deliberate choice of $\Delta\omega$. Suppose for simplicity $\phi_0(\xi)\phi_1^*(\xi) = F$ for $0 \le \xi \le L$ and $-F$ for $-L \le \xi \le 0$. The wake amplitude is evaluated as $|\phi_p(x,\infty)|^2 = \text{const.}\ \sin^2\left[\left(\Delta\tilde{\omega} + \tilde{\Lambda}_{\text{av}}\right)L/2\right]$, where $\tilde{\Lambda}_{\text{av}} = \int_{-L}^{L} \Lambda d\xi/2L$. The wakeless condition is achieved when $\Delta\omega = -3\omega_p\,|\phi_p|^2_{\text{av}}/16$, where $|\phi_p|^2_{\text{av}} = \int_{-L}^{L} d\xi|\phi_p(\xi)|^2/2L$.

To investigate the robustness of this triple soliton acceleration mechanism, we carry out two kinds of numerical experiments. The first is direct numerical integration of Eqs. (1)-(3). The second is self-consistent electromagnetic particle simulation. Figures 1(b)-(d) show the direct integration of Eqs. (1)-(3) with initialization Eqs. (7)-(9). Because of the relativistic detuning in (b) and the frequency mismatch in (d) there is no annihilation of the wake. Large amplitude wakes are emitted from the trisoliton initial condition in Figs. 1(b) and (d). In Fig. 1(c), however, when the frequency mismatch is chosen appropriately to cancel the relativistic detuning, we observe the wakeless trisoliton propagate very stably. In this case, $|\phi_p|^2_{\text{av}}$ of the wakeless condition is found to be 0.4 times the peak intensity. Overall, we find the relativistic trisoliton can propagate stably in spite of the relativistic

nonlinearity.

We further investigate kinetic effects on the trisoliton. In Fig. 2 we show the results of a particle simulation. In contrast to the first numerical integration, we start with Eqs. (7) and (8) for electromagnetic waves but with $\phi_p \cong 0$ [not Eq. (9)], because of the nature of the particle simulation. The structure at early time $t = 12.5\omega_p^{-1}$ after the two tailored laser beams are injected resembles the anticipated profiles Eqs. (7)-(10). Note also the substantial electron forward momentum created by the accelerating electrostatic field [Fig. 2(d)]. At this time the electron plasma wave is localized around $x = 100\Delta$. At $t = 50\omega_p^{-1}$, the plasma wave is around $x = 500\Delta$ as seen in Fig. 2. This corresponds to the velocity of the electrostatic wave of $\sim 0.9c$, much faster than the group velocity of the plasma wave. However, in this simulation the plasma wavepacket speed is still slightly less than c; thus the wake creation is much reduced but remains. The difference of the simulation result from the ideal case Eq. (9) may be due to the effective dissipation of the plasma wave from the acceleration of the thermal electrons shown in Fig. 2(e). In addition, it may be the phase mismatch occurring from the accelerated electrons, or the non-ideal start of the electrostatic wave amplitude, ϕ_p, which does not satisfy Eq. (9).

If we insist on the exact wakeless condition at λ=c, according to Eq. (10), the accelerating electric field E_p is $(\omega_p/\omega_0)^{3/2}E_0$. In order to maintain a large accelerating field, we want to keep ω_p/ω_0 not too small. On the other hand, the energy ε of the trapped electron in the electrostatic wave scales[2] in the beat-wave accelerator as $\varepsilon \sim 2mc^2(\omega_0/\omega_p)^2$, which is in conflict with the above relation. In order to overcome this dilemma, it is important to control the phase velocity of the accelerating electrostatic field E_p. However, if one can make the phase velocity $v_p \to c$, this restriction of $\varepsilon \propto (\omega_0/\omega_p)^2$ disappears and an indefinite acceleration appears possible except as limited by pump depletion and beam loading. This condition v_p=c can be realized in a plasma fiber, in which the plasma density is low in the middle for laser propagation and high toward the edge. The plasma fiber at the same time acts to trap the laser beams within it so that the pump field does not spread

out. Consider a two-dimensional rectangular configuration in which the plasma density n inside the fiber is constant width d and the outside density is $n'(> n)$. We find that the phase velocity of the accelerating plasma wave can be made to be the speed of light c if an appropriate size of the fiber width is chosen. We can see this as follows. We demand the frequency matching among the two laser beams and the plasma wave $\omega_0 - \omega_1 = \omega_p$, as before. Further, we require the parallel phase velocity of the plasma wave be the speed of light $(\omega_0 - \omega_1)/(k_{\|0} - k_{\|1}) = c$, where $k_{\|j} = [\omega_j^2/c^2 - \omega_p^2/c^2 - (\pi\ell_j/d)^2]^{1/2}$ where ℓ_j is the number of transverse mode in the fiber. If we choose $\ell_0 = \ell_1 + 1$, $\ell_1 = 1$, and $\omega_0/\omega_p >> 1$, we arrive at the condition for the fiber width for the indefinite acceleration $d = \sqrt{3}\,\dfrac{\pi c}{\omega_p}\left(\dfrac{\omega_0}{\omega_p}\right)^{1/2}$.

Figure 3 shows the test of this idea by the self-consistent fully relativistic electromagnetic particle simulation. We allow plasma particles outside of the fiber initially 10 times as dense as that in the fiber which runs in the y-direction parallel to the laser injection direction. Figure 3 is the case with E_x plane polarized laser electric fields with a flat wave amplitude. The electrostatic potential of the beat plasma wave is shown in Fig. 3(a) after time $t\omega_{p0}$=8. The electrostatic potential structure represents the beat-wave created by the ponderomotive force as previously discussed.[2] The laser lights have remained confined in the fiber. The initial duct width is indicated by the two marks on the x axis. The contours of the electrostatic potential show the structure of the beat-wave which clearly has the difference wavenumber, $k_{\rm beat} = k_0 - k_1 = 2\pi \times 7/128\Delta$. The phase velocity of the plasma wave is measured in Fig. 3(b): v_{ph}(measured) $= 2.942\omega_{po}\Delta$. This is very close to the speed of light $c = 2.909\omega_{po}\Delta$, in agreement with the idea presented here. The phase velocity measured without the fiber structure was such that $(v_{ph} - c)/c \simeq 0.0670$, which approximately corresponds to $\dfrac{1}{2}(\omega_p/\omega)^2$ as expected. On the other hand, with the fiber $|c - v_{ph}|/c \simeq 0.01$, which is within the measurement error of $v_{ph} = c$.

With the wakeless triple soliton in a plasma fiber under the appropriate conditions discussed above we have achieved: (i) the phase velocity of the accelerating plasma wave is

c with laser beams trapped in the fiber; (ii) the entire envelope structure of the two laser beams and the beat plasma wave forms a wakeless triple soliton whose propagation velocity is again c. The latter velocity may be called the effective velocity of the driven plasma wave soliton. Thus, our concept realizes both the phase velocity and the effective velocity of the structure of the accelerating plasma wave profile to become close to the accelerated particle velocity under the appropriate conditions. Hasegawa has considered an optical fiber soliton,[8] a single soliton, not a triple soliton. Although the acceleration length of our concept is theoretically infinite, the practical length is limited by beam loading.[9]

Acknowledgment

This work was supported by The National Science Foundation and Department of Energy contract #DE-FG05-80ET-53088, and the Texas Acceleration Center Grant TAC 85100.

References

1. C. Rubbia, invited talk in *The Generation of High Fields*, Proceedings of the CAS-ECFA-INFN Workshop, eds. P. Bryant and J. Mulvey (INFN, Frascati, 1984) p. vi.
2. T. Tajima and J.M. Dawson, Phys. Rev. Lett **43**, 267 (1979).
3. S.L. McCall and E.L. Hahn, Phys. Rev. **183**, 457 (1969).
4. V.E. Zakharov, Sov. Phys. JETP **35**, 908 (1972) [Zh. Eksp. Teor. Fiz. **62**, 1745 (1972)].
5. M.N. Rosenbluth and C.S. Liu, Phys. Rev. Lett. **29**, 701 (1972).
6. W. Horton and T. Tajima, AIP Conference Proceedings on Laser Acceleration of Particles, Malibu, California, 1985, ed. by C. Joshi and T. Katsouleas, American Institute of Physics, p. 179, 1985.
7. K. Nozaki and T. Taniuti, J. Phys. Soc. Jpn. **34**, 796 (1973).
8. A. Hasegawa, Opt. Lett. **9**, 288 (1984).
9. Beam loading power at the maximum acceleration phase is $P_b = e \langle n_b \rangle v_b E_{p\max}$, with $\langle n_b \rangle$ being the average beam density. The depletion time of the plasma wave is $\tau_b = \langle E_p^2 \rangle / 4\pi P_b = n_0 a_p / (\omega_p \langle n_b \rangle c)$. The acceleration length with beam loading, $L_{\rm acc} = \tau_b c$ is much longer than the dephasing length, $2\gamma_\phi^2 c/\omega_p$, if $\langle n_b \rangle / n_0 \ll a_p/(2\gamma_\phi^2 c)$.

Figure Captions

Fig. 1: Numerical integration results. Amplitude profiles of two electromagnetic waves (thick solid lines; $\omega_0/\omega_p = 6.0$, broken lines; $\omega_1/\omega_p = 5.0$) and the beat electron plasma wave (thin solid lines). The initial soliton amplitude is $a = v_0/c = 1.0$, $a_p = \delta n_p/n_0$. The laser pulse length is finite ($\sim 6c/\omega_p$). (a) Initial profiles at t=0 the pump wave amplitude is zero in the region far from the soliton. (b),(c) and (d) are the profiles at t=$88\omega_p^{-1}$ for $\Delta\omega/\omega_p = 0$, $-0.4\Lambda_{\max}$ and $-1.0\Lambda_{\max}$ respectively, where $\Lambda_{\max}$ is the relativistic frequency shift at the maximum amplitude.

Fig. 2: Particle simulation results. Typical parameters of the simulations are system length $L_x = 2058\Delta$, $c = 10\omega_0\Delta$, $\omega_0/\omega_p = 6.3$, $\omega_1/\omega_p = 5.3$, $\Delta\omega \cong 0$, $a = v_0/c = 0.6$, $v_e = 0.6\omega_p\Delta$, which would make λ close to c. (a) Schematic trisoliton. The laser is immersed in a plasma at t=0 for the phase jump at x=0 (propagating toward $+x$ direction). (b) and (c) at t=$12.5\omega_p^{-1}$, (d), (e) and (f) at t=$50\omega_p^{-1}$. (b) and (e) The plasma electric field amplitude vs. x. (c) and (f) The laser field amplitude vs. x, (d) the electron phase space p_x vs. x.

Fig. 3: Beat-wave in the plasma fiber. The density profile has a duct width, $d = 22.05\Delta$ and $n'/n = 10$, the original wavenumbers are $k_0 = 2\pi \times 22/128\Delta$ and $k_1 = 2\pi 4/5/128\Delta$, the speed of light $c = 2.909\omega_{p0}\Delta$, the quiver velocity of the light waves $v_{osj} = 0.6c(j = 0 \text{ and } 1)$ and $v_p = 0.5\omega_{p0}\Delta$, where ω_{p0} is the plasma frequency in the duct and Δ is the grid spacing. (a) Electrostatic potential contour profile: stratified wave fronts appear within the fiber ($8\omega_{p0}^{-1}$). (b) Phase progression of the beat plasma wave in time. The solid line indicates y=ct.

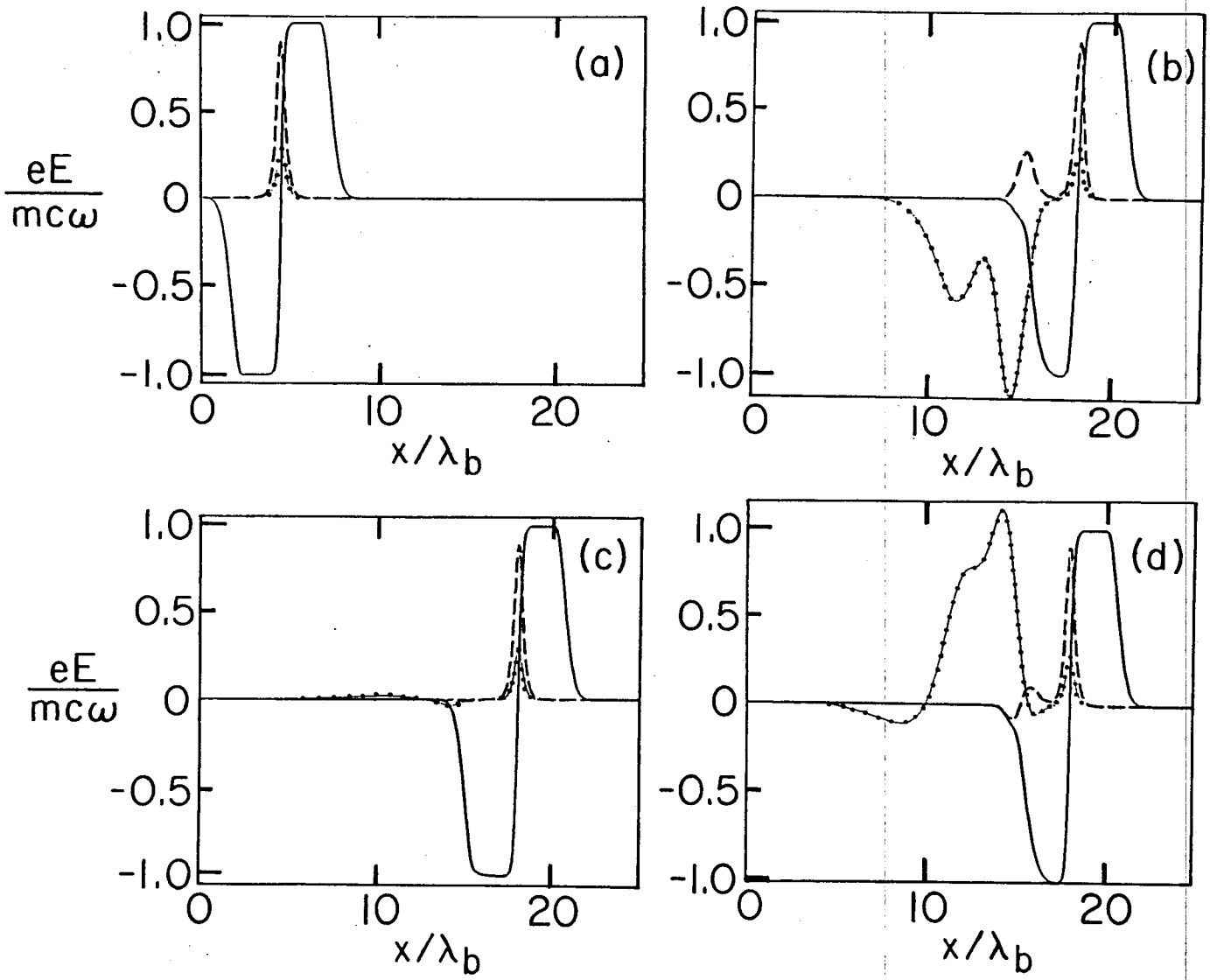

Fig. 1

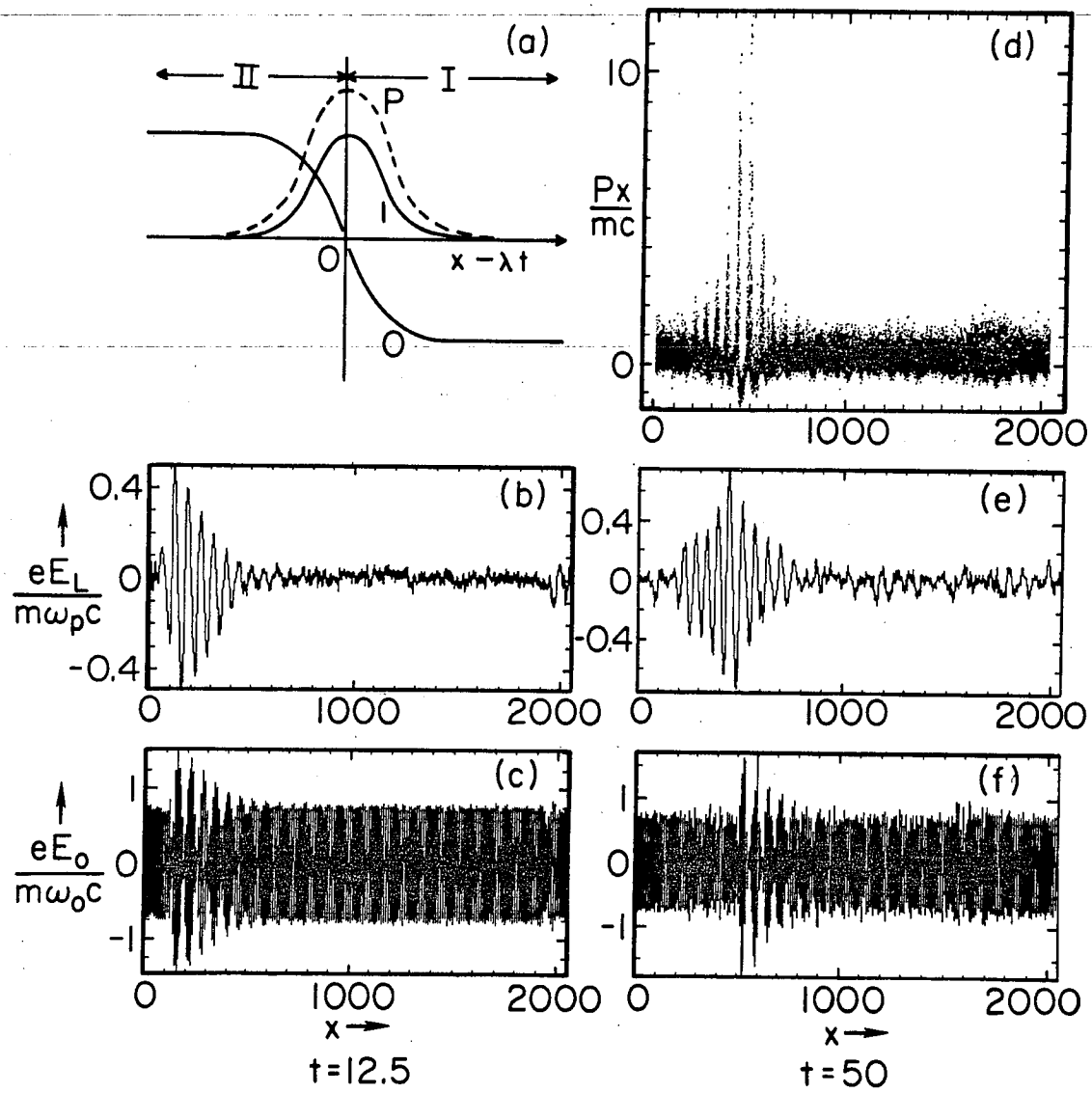
(a)
II
I
P
I
0
x − λt
0
(d)
10
Px/mc
0
0
1000
2000
(b)
0.4
eE_L/mω_pc
0
-0.4
0
1000
2000
(e)
0.4
0
-0.4
0
1000
2000
(c)
1
eE_0/mω_0c
0
-1
0
1000
2000
x
t=12.5
(f)
1
0
-1
0
1000
2000
x
t=50

Fig. 2

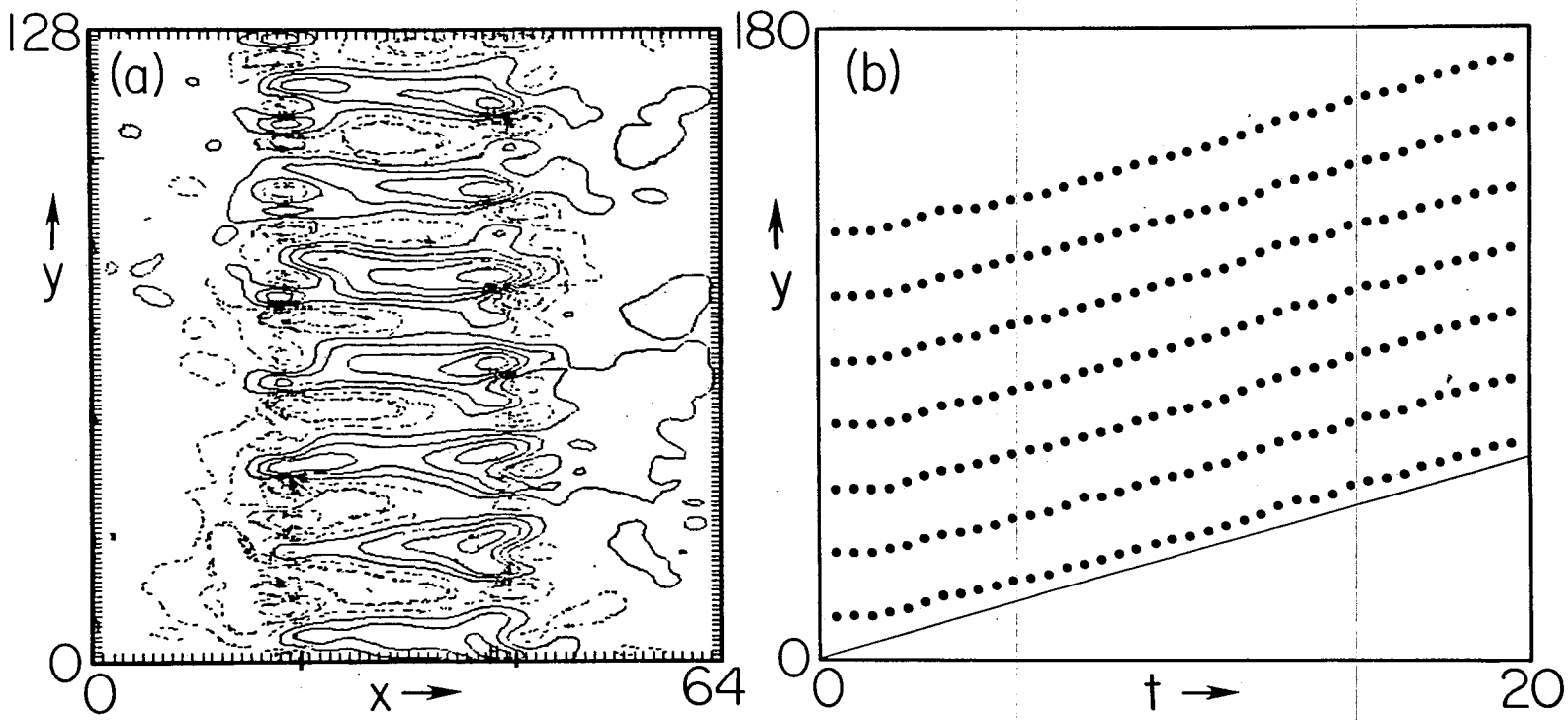

Fig. 3